Charge Induced $\chi^{(3)}$ Susceptibility in Interfacial Nonlinear Optical Spectroscopy Beyond the Bulk Aqueous Contributions: The Case for Silica/Water Interface

Hui Wang,[†] Xiao-Hua Hu,[†] and Hong-Fei Wang[*,†,‡,#]

[†]Department of Chemistry, Fudan University, 220 Handan Road, Shanghai 200433, China.
[‡]School of Sciences, Westlake University, 18 Shilongshan Road, Hangzhou 310024, Zhejiang Province, China.
[#]Institute of Natural Sciences, Westlake Institute for Advanced Study, 18 Shilongshan Road, Hangzhou 310024, Zhejiang Province, China.

* Corresponding Author.

E-Mail: wanghongfei@westlake.edu.cn

ORCID

Hui Wang: 0000-0003-1039-7833

Xiao-Hua Hu: 0000-0002-4839-5000

Hong-Fei Wang: 0000-0001-8238-1641

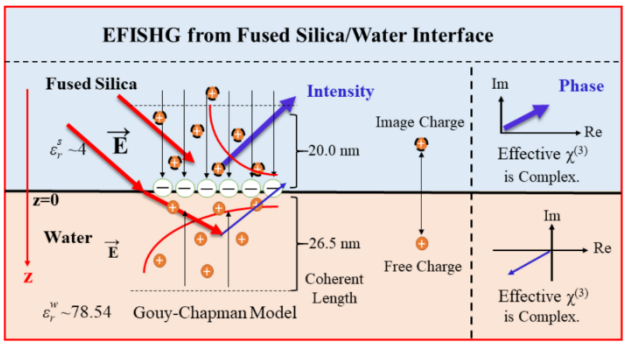

Table of Contents (TOC)

ABSTRACT

The electric field induced (EFI) bulk $\chi^{(3)}$ contribution to the second harmonic generation (SHG) signal from charged interfaces was discovered and applied to study the interfacial chemistry of various charged interfaces three decades ago. For both the buried fused silica/water interface and the exposed charged monolayer covered air/water interface, such bulk $\chi^{(3)}$ contribution was all attributed to the $\chi^{(3)}$ term of the polarized water molecules near the charged interfaces. The puzzling experimental observation of the more than one-order of magnitude difference of the EFISHG intensity between the fully charged silica/water interface and the charged molecular covered air/water interface was generally overlooked in the EFISHG literature. Nevertheless, this significant signal difference suggests additional source for the $\chi^{(3)}$ contribution at the fully charged silica/water interface other than the polarized water molecules as in the case of charged monolayer covered air/water interface. In this report, we re-examine the treatment of the $\chi^{(3)}$ mechanism at the charged silica/water interface by including the contributions from the bulk silica using proper boundary condition and image charge distributions for the change screening effects inside bulk silica phase. We show that the $\chi^{(3)}$ contribution from the bulk silica is in similar form as that of the aqueous bulk phase, and it is with more than one-order of magnitude and with opposite sign. The treatment reported here can be extended to other charged interfaces.

1. INTRODUCTION

Charged interface commonly exist in nature and biological system, responsible for heterogeneous processes and interfacial phenomena important in many geological, environmental, electrochemical, biological, and industrial systems. Using electric field induced second harmonic generation (EFISHG) or sum-frequency generation vibrational spectroscopy (SFG-VS), one can directly measure the potential changes across the charged interfaces through the bulk $\chi^{(3)}$ mechanism first demonstrated by Eisenthal et al. in the early 1990s.[1-3] The two typical charged interface systems studied were the silica/water interface and the charged Langmuir monolayer covered air/water interface. It was successfully shown that the second harmonic field responses from those interfaces are linearly dependent on the interfacial electric potential, making it possible to directly and quantitatively study the electrolyte concentration effects and acid-base equilibrium at the charged aqueous interfaces.[1-3]

In these studies, the bulk $\chi^{(3)}$ contributions to the interfacial SHG signal were all attributed to the polarized water molecules near the charged interfaces. This treatment does not cause problem if the change of the detected SHG field linearly depends on the interfacial potential, and this relationship was still effective to extract information of the interfacial potential. The fact that the more than one orders of magnitude difference between the SHG signal from the fully charged silica/water interface and the fully charged Langmuir monolayer cover air/water interface is generally overlooked.

For the positively charged ($CH_3(CH_2)_{21}N(CH_3)_3Br$) monolayer at air/water interface,[2] when the charge density decreased from 0.32 to 0.08 C/m^2, i.e., from 50 to 200 $\AA^2$/per charge, the SHG field $E_{2\omega}$ changed from 2.0 to 1.7, assuming the neat air/water value is unity; while for negatively charged

monolayer ($CH_3(CH_2)_{21}SO_3K$), the SHG field in the same charge density range changed from 0.5 to 0.85. In the case of monolayer $CH_3(CH_2)_{21}NH_2$ amine at air/water interface,[3] the $E_{2\omega}$ increased from 0.9 to 2.4 as the bulk pH change from 12 to 2, corresponding to the change of the fully neutral $CH_3(CH_2)_{21}NH_2$ monolayer to the fully positively charged $CH_3(CH_2)_{21}NH_3^+$ monolayer. These results suggested that the charge induced $\chi^{(3)}$ contributions to the total SHG field when the interface is fully charged is comparable to that of the neat air/water interface.

In comparison, for the fused silica/water interface,[1] as the interfacial charge density increased with the bulk pH value from 2.0 (nearly neutral surface) to 12.7 (fully negatively charged with surface charge density of 0.87 x 10^{14}/cm^2 or 115 $\AA^2$/per charge), the SHG field $E_{2\omega}$ increased from 5 to 52, a ten-fold increase. As the neutral silica/water interface SHG signal is already significantly larger than that of the neat air/water interface, the ten-fold increase of the SHG field, as the interface becomes fully charged at high pH, cannot be reasonably attributed to the charge induced $\chi^{(3)}$ contributions from the polarized water molecules near the silica/water interface, as in the case of the monolayer covered air/water interface with comparable surface charge density, mentioned above.

The major difference between the silica/water interface and the air/water interface is that in the former case there are two adjacent bulk phases, i.e., the silica phase and the water phase; while in the latter case, there is only one bulk phase, i.e., the water phase. Therefore, it is natural to conclude that the significantly different level of the EFISHG signal of the charged silica/water interface from that of the charged air/water interface is the result of the contribution of the charge induced $\chi^{(3)}$ contributions from the silica phase. Moreover, from the experimental data, it is not difficult to see that this contribution is the dominant part in the charged silica/water interface EFISHG signal, which has been overlooked in the treatment of the silica/water interface EFISHG so far.

A recent report by Hore and Gibbs et al. systematically examined the significant differences between the pH dependent behavior of the silica/water interface measured by non-resonant SHG and sum-frequency generation vibrational spectroscopy (SFG-VS).[4] They pointed out that silica substrate contributes significantly to the SHG signal but not to the SFG-VS signal because unlike the water molecules, silica is not vibrationally in resonance with the SFG-VS. However, as they focused on the $\chi^{(2)}$ changes at the silica/water interface, the possible charge induced $\chi^{(3)}$ contributions to SHG from the silica phase was not discussed. As we shall show in this report, since the bulk silica phase contributes dominantly to the overall $\chi^{(3)}$ signal in SHG, many issues discussed in their report on the SHG response from the silica/water interface can be satisfactorily addressed by considering the charge induced $\chi^{(3)}$ contributions from the silica phase.

There has been a recent revival of the studies on the often overlooked charge induced $\chi^{(3)}$ contributions from the polarized bulk water molecules near the charged interface to the SHG and SFG signal.[5-7] The main focus of these studies are trying to quantitatively understand the phase-resolved SFG-VS spectra of the charged aqueous interface[5] and to address the phase referenced SHG measurement data of the quartz/water interface.[7] These efforts not only led to the corrected description of the charge induced $\chi^{(3)}$ contributions of the polarized water molecules in general,[5-7] but also resulted to a series systematic treatment of the spectral lineshapes of the phase-resolved SFG-VS spectra of the charged aqueous interfaces involving the $\chi^{(3)}$ contributions from polarized bulk water molecules near the charged interface.[8-14] With the explicit definition of the two phase angles, one of the charge induced $\chi^{(3)}$ term and another between the $\chi^{(3)}$ and the $\chi^{(2)}$, which are both experimentally measurable,[12] Geiger and co-workers recently discovered that for the SHG from the charged silica/water interface there exists an additionally new imaginary non-resonant

$\chi^{(3)}$ term other than the traditionally considered $\chi^{(3)}$ contributions from polarized bulk water molecules near the charged interface.[15] We shall show that the $\chi^{(3)}$ contributions from the bulk phase is actually complex and likely more complicated than what has been considered. Further investigation to quantitatively measure and interpret the phase resolved EFISHG data is warrantied in future studies.

2. PHASE-RESOLVED $\chi^{(3)}$ CONTRIBUTIONS FROM BULK AQUEOUS PHASE

The SHG response from a charged aqueous solution interface includes contributions from the second-order susceptibility of the interfacial layer ($\chi^{(2)}$) and the third-order susceptibility of the polarized bulk water molecules near the charged interface ($\chi^{(3)}E_0(z)$) within the coherent length of the SHG process ($1/\Delta k_z$). In previous literature, only the $\chi^{(3)}$ contribution from the polarized bulk water molecules near the charged interface is considered. After consideration of the charge screening effects in the aqueous phase and the coherent length of the SHG process,[6] the overall SHG field from a charged aqueous interface can be expressed as,[7, 9]

$$\begin{aligned} E_{2\omega} &\propto \chi^{(2)}E_\omega E_\omega + \chi^{(3)}\frac{\kappa}{\kappa - i\Delta k_z}\Phi(0)E_\omega E_\omega \\ &= \chi^{(2)}E_\omega E_\omega + \chi^{(3)}\left[\frac{\kappa^2}{\kappa^2+\Delta k_z{}^2} + \frac{i\Delta k_z\kappa}{\kappa^2+\Delta k_z{}^2}\right]\Phi(0)E_\omega E_\omega \end{aligned} \tag{1}$$

or,

$$\chi^{(2)}_{total} = \chi^{(2)}_{surface} + [\chi^{(3)}_1 + i\chi^{(3)}_2]\Phi(0) = \chi^{(2)} + \chi^{(3)}\Phi(0)\cos\varphi e^{i\varphi} \tag{2}$$

where $\chi^{(n)}$ is the nth-order nonlinear susceptibility, E_ω is the incident optical field of photon with frequency ω; $1/\Delta k_z = 1/\left|\vec{k}_{1z} + \vec{k}_{1z} - \vec{k}_{0z}\right| = 1/(k_{1z} + k_{1z} + k_{0z})$ is the coherent length,[24-27] with $k_{iz} = \omega_i / c\sqrt{n(\omega_i)^2 - \sin(\theta_i)^2}$; $1/\kappa$ is the Debye screening length of the electrolyte aqueous solution; and $\Phi(0)$ is the surface potential of the charged interface, $\varphi = \arctan(\Delta k_z^w / \kappa_w)$ is the phase

between the $\chi^{(2)}$ and $\chi^{(3)}$.[12] The term $\frac{\kappa}{\kappa - i\Delta k_z} = \frac{\kappa^2}{\kappa^2 + \Delta k_z^{\,2}} + \frac{i\Delta k_z \kappa}{\kappa^2 + \Delta k_z^{\,2}}$ in eq1 defines the real and imaginary coefficients of the bulk $\chi^{(3)}$ contributions, with $\chi_1^{(3)} = \frac{\kappa^2}{\kappa^2 + \Delta k_z^{\,2}} \chi^{(3)}$, $\chi_2^{(3)} = \frac{i\Delta k_z \kappa}{\kappa^2 + \Delta k_z^{\,2}} \chi^{(3)}$ in eq 2. When $\Delta k_z / \kappa \gg 1$, one has $\chi_1^{(3)} - i\chi_2^{(3)} \sim i\chi_2^{(3)}$, indicating that the $\chi^{(3)}$ contribution is nearly pure imaginary; while when $\Delta k_z / \kappa \ll 1$, one has $\chi_1^{(3)} - i\chi_2^{(3)} \sim \chi_1^{(3)}$, indicating that the $\chi^{(3)}$ contribution is nearly real. Therefore, the $\chi^{(3)}$ contribution is real when the coherent length $1/\Delta k_z$ of the SHG process is larger than the Debye length $1/\kappa$; and vice versa. Physically, the coherent length of the SHG response ($1/\Delta k_z$) defines the region near the interface that is probed with SHG. If the SHG probes the whole region across the range of the electric field in the diffuse layer (DL) quantified by the Debye length, the detected $\chi^{(3)}$ contribution is real; otherwise, partial probe of this region makes the detected $\chi^{(3)}$ contribution a complex quantity.

Initially, the treatment of $\chi^{(3)}$ contribution did not consider the effects of the effective probing length defined by the coherent length of the SHG process or the phase matching factor $e^{i\Delta k_z z}$.[1-2, 16] Then the whole $\chi^{(3)}$ contribution was real and it cannot satisfactorily interpret the phase-resolved SHG data.[7] If only the phase matching factor $e^{i\Delta k_z z}$ of the SHG process is considered without including the charge screening effects defined with the Debye screening length, the bulk $\chi^{(3)}$ contribution term is going to be pure imaginary.[8, 17] This is can be seen in one case for the bulk silica $\chi^{(3)}$ contribution to be discussed below.

3. $\chi^{(3)}$ CONTRIBUTIONS FROM BOTH SILICA AND WATER PHASES

SHG and SFG-VS has been used extensively in studying the charged silica/water interface.[1, 4, 14, 18-27] The interpretations based on non-resonant SHG and SFG-VS data and by considering of the $\chi^{(3)}$

contributions exhibited substantial disagreements and have been puzzling the community.[4, 15] After reviewing the significantly different SHG signal data from the charged silica/water and the charged Langmuir monolayer covered air/water interface,[1-3] the necessity to consider the bulk silica $\chi^{(3)}$ contributions at the charges silica/water interface was recognized, and the details are yet to be hammered out.[8] The most recent phase-resolved SHG measurement of the silica/water interface also called for an additional new imaginary $\chi^{(3)}$ term ($\chi_X^{(3)}$) to go beyond the existing $\chi^{(3)}$ model, as expressed in eq 3, which considers only the contributions from the polarized bulk water molecules.[15] An attempt to consider the bulk silica phase to account for the $\chi_X^{(3)}$ term was unsuccessful, and was abandoned.

$$\chi_{total}^{(2)} = \chi_{surface}^{(2)} + [\chi_1^{(3)} - i\chi_2^{(3)} \pm i\chi_X^{(3)}]\Phi(0) \quad (3)$$

These all call for a treatment that may address these issues. Below we present a unified treatment of the $\chi^{(3)}$ contributions from both the bulk silica and water phases to the charged silica/water interface.

3.1 Charged Interface Between Two Bulk Dielectric Solid Phases

The simplest model for charged interface can be treated as a sheet of charges with a uniform charge density of σ. This interface charge induces polarization in the bulk phase on both sides. We consider the charged interface between two dielectric solid phases, in which no free charge exists and therefore no charge screening would be created by the charged interface near the interface of the electrolyte aqueous phase. Figure 1 shows the negatively charged interface, i.e., σ is negative, between the two solid phases with dielectric constant ε_r^I and ε_r^{II}. According to the Gauss Theorem of electromagnetism, the static electric fields created by the interfacial charge in the two solid phases

are $E_I^0 = -\frac{\sigma}{\varepsilon_0 \varepsilon_r^I}$ and $E_{II}^0 = \frac{\sigma}{\varepsilon_0 \varepsilon_r^{II}}$, respectively. Here, the superscript 0 denotes the zero frequency for the static field. The important thing here is that, in the lossless dielectric phase I and II, E_I^0 and E_{II}^0 are both distance independent. Therefore, the total SHG field response is,

$$E_{2\omega}^{total} = \chi_{eff}^{(2)} E_\omega E_\omega = \left(\chi^{(2)} + \chi_{I,eff}^{(3)} + \chi_{II,eff}^{(3)} \right) E_\omega E_\omega \tag{4}$$

with the $\chi^{(3)}$ contributions from the two phases as,

$$\chi_{I,eff}^{(3)} = \int_{-\infty}^{0^-} \chi_I^{(3)} E_I^0 e^{-i\Delta k_I z} dz = -\frac{\chi_I^{(3)} E_I^0}{i\Delta k_I} = i\chi_I^{(3)} E_I^0 l_c^I = -i\frac{\chi_I^{(3)} \sigma}{\varepsilon_0 \varepsilon_r^I} l_c^I \tag{5}$$

$$\chi_{II,eff}^{(3)} = \int_{0^+}^{\infty} \chi_{II}^{(3)} E_{II}^0 e^{i\Delta k_{II} z} dz = -\frac{\chi_{II}^{(3)} E_{II}^0}{i\Delta k_{II}} = i\chi_{II}^{(3)} E_{II}^0 l_c^{II} = i\frac{\chi_{II}^{(3)} \sigma}{\varepsilon_0 \varepsilon_r^{II}} l_c^{II} \tag{6}$$

in which $l_c^I = 1/\Delta k_I$ and $l_c^{II} = 1/\Delta k_{II}$ are the coherent lengths of the SHG process in Phase *I* and Phase *II*, respectively. The phase factor $e^{-i\Delta k_I z}$ and $e^{i\Delta k_{II} z}$ in eqs 5 and 6 take opposite phases because the interface is in the opposite direction of the two bulk phases. Here the evaluation of the integration in eqs 5 and 6 followed the standard procedure when considering integration of the phase factor to the infinity.[17] Because any dielectric bulk medium is not completely lossless, therefore, physically the optical wave would converge to zero when approaches to infinity. Then the total SHG response from this charged interface is,

$$\begin{aligned} E_{2\omega}^{total} &= \chi_{eff}^{(2)} E_\omega E_\omega \\ &= \left(\chi^{(2)} + i\chi_I^{(3)} E_I^0 l_c^I + i\chi_{II}^{(3)} E_{II}^0 l_c^{II} \right) E_\omega E_\omega \\ &= \left(\chi^{(2)} + i\sigma \left(-\frac{\chi_I^{(3)} l_c^I}{\varepsilon_0 \varepsilon_r^I} + \frac{\chi_{II}^{(3)} l_c^{II}}{\varepsilon_0 \varepsilon_r^{II}} \right) \right) E_\omega E_\omega \end{aligned} \tag{7}$$

or,

$$\begin{aligned} \chi_{eff}^{(2)} &= \chi^{(2)} + i\chi_I^{(3)} E_I^0 l_c^I + i\chi_{II}^{(3)} E_{II}^0 l_c^{II} \\ &= \chi^{(2)} + i\sigma \left(-\frac{\chi_I^{(3)} l_c^I}{\varepsilon_0 \varepsilon_r^I} + \frac{\chi_{II}^{(3)} l_c^{II}}{\varepsilon_0 \varepsilon_r^{II}} \right) \end{aligned} \tag{8}$$

Here eqs 7 and 8 give the total SHG response from the charged interface between two solid dielectric phases. The $\chi^{(3)}$ contributions from the two bulk solid phases are with opposite signs, and both are proportional to the interface charge density σ. The $\chi^{(3)}$ contributions are pure imaginary terms against the interfacial susceptibility $\chi^{(2)}$. The value of the $\chi^{(3)}$ contribution from each bulk phase i is proportional to its bulk third order susceptibility $\chi_i^{(3)}$, the SHG coherent length l_c^i, the interfacial charge density, and inversely proportional to its dielectric constant ε_r^i. The simple relationship in eqs 7 and 8 can allow explicit SHG measurement of interfacial charge density, which is a linear function of the total SHG response.

Such simple relationship is the results of the fact that the bulk solid dielectric phases are free from charge screening. This would not be valid for the bulk electrolyte aqueous phase near the charged interface, e.g., the silica/water interface, or any bulk material that charge distribution can be affected by the presence of the interfacial charge.

Let's suppose that there is no charge screening in the aqueous phase. Then, because the aqueous phase has a static dielectric constant of 78.54 and the static dielectric constant of the silica phase is about 4, the $\chi^{(3)}$ contributions from the bulk silica phase can be about 20 times of that from the aqueous phase, if their bulk $\chi_i^{(3)}$ and l_c^i values are comparable just because of the huge difference of their static dielectric constant. Moreover, when there is charge screening in the aqueous phase, the electric field in the aqueous phase near the charged interface would decay faster with the distance from the interface increase than that without. Subsequently, the $\chi^{(3)}$ contribution from the aqueous phase is expected to be smaller in comparison to that without the charge screening effects. The $\chi^{(3)}$ contribution from the aqueous phase with the charge screening effects has been satisfactorily treated.[7] However, the charge screening in the aqueous phase can also cause reduction of the field

strength in the silica phase. These facts can further complicate the treatment of the $\chi^{(3)}$ contributions from the bulk silica phase.

The simple model discussed here without charge screening is probably unphysical. Nevertheless, it provides important physical insight to understand the interfacial potential and fields, as well as the bulk $\chi^{(3)}$ contributions induced by these fields. We have been used to the expression of the $\chi^{(3)}$ contributions in terms of the interfacial potential $\Phi(0)$. However, in eqs 7 and 8, there is no potential term. Instead, the field times the coherent length with the same dimension unit replaces it. For a lossless dielectric media extended to infinite, it is impossible to define the interfacial potential $\Phi(0)$. Even though this indicates that the model itself is unphysical or at most a simplified model, it can still be treated quantitatively using the field term and the coherent length. More importantly, the discontinuity of the fields across the interface can be unambiguously defined using the Gauss Theorem. These facts suggest to us that in describing the bulk $\chi^{(3)}$ contributions, the fields in the interface region are primary and explicit than the interfacial potential.

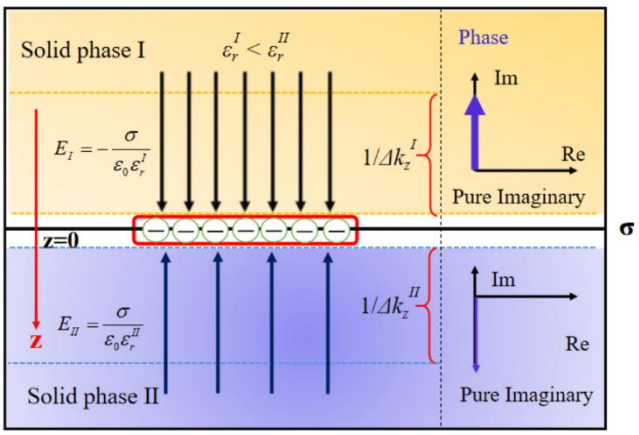

Figure 1. The electric fields on both sides of the interface for negative charged interface with interfacial charge density σ, without free charge in the bulks. The red and black arrows represent the direction of z and electric field E. The electric fields are constant and inversed proportion to dielectric constant ε_r, $1/\Delta k_z$ is the coherent length of the interfacial SHG process. The resulted bulk $\chi^{(3)}$ contributions are both pure imaginary with opposite signs.

3.2 $\chi^{(3)}$ Treatment of the Silica/water interface

Following eq 4, by including the $\chi^{(3)}$ contributions from the bulk silica and water phases, the total SHG response at the silica/water interface is,

$$E_{2\omega}^{total} = \chi_{eff}^{(2)} E_\omega E_\omega = \left(\chi^{(2)} + \chi_{s,eff}^{(3)} + \chi_{w,eff}^{(3)}\right) E_\omega E_\omega \tag{9}$$

with,

$$\chi_{s,eff}^{(3)} = \int_{-\infty}^{0^-} \chi_s^{(3)} E_s^0(z) e^{-i\Delta k_s z} dz = \int_{-\infty}^{0^-} \chi_s^{(3)} \left(-\frac{d\Phi_s(z)}{dz}\right) e^{-i\Delta k_s z} dz \tag{10}$$

and,

$$\chi_{w,eff}^{(3)} = \int_{0^+}^{\infty} \chi_w^{(3)} E_w^0(z) e^{i\Delta k_w z} dz = \int_{0^+}^{\infty} \chi_w^{(3)} \left(-\frac{d\Phi_w(z)}{dz}\right) e^{i\Delta k_w z} dz \tag{11}$$

Here, the subscripts *s* and *w* represent silica and water phase properties, respectively. Eq 11 follows the treatment for charge screening and coherent length effects in the bulk aqueous phase. Therefore, the static electric field $E_w^0(z)$ in the aqueous phase is distance dependent, and the potential in the bulk water phase can be treated as $\Phi_w(z) = \Phi_w(0) e^{-\kappa_w |z|}$.[7]

Here we need to discuss the following two different scenarios.

The first scenario (Figure 3) assumes that the silica phase is independent from the charge screening in the aqueous phase. This is a simplified picture, to be shown below. Nevertheless, it can provide certain physical insight to start with. Accordingly, eqs 10 and 11 give,

$$\chi_{s,eff}^{(3)} = \int_{-\infty}^{0^-} \chi_s^{(3)} E_s^0 e^{-i\Delta k_z^s z} dz = -\frac{\chi_s^{(3)} E_s^0}{i\Delta k_z^s} \tag{12}$$

$$\begin{aligned} \chi_{w,eff}^{(3)} &= \chi_w^{(3)} \frac{1}{1 - i\Delta k_z^w / \kappa_w} \Phi_w(0) \\ &= \chi_w^{(3)} \left[\frac{\kappa_w^{\,2}}{\kappa_w^{\,2} + (\Delta k_z^w)^2} + \frac{i\Delta k_z^w \kappa_w}{\kappa_w^{\,2} + (\Delta k_z^w)^2}\right] \Phi_w(0) \end{aligned} \tag{13}$$

and the Gauss Theorem gives the boundary condition $\varepsilon_r^s E_0^s = \varepsilon_r^w E_0^w(0)$ at the interface, i.e.,

$$\varepsilon_r^s E_0^s = \varepsilon_r^w E_0^w(0) = \varepsilon_r^w \left(-\frac{d\Phi_w(z)}{dz}\right)_{z=0} = \varepsilon_r^w \kappa_w \Phi_w(0) \tag{14}$$

Therefore,

$$\chi_{eff}^{(2)} = \chi^{(2)} + \left(i\chi_s^{(3)} \frac{\kappa_w(\varepsilon_r^w / \varepsilon_r^s)}{\Delta k_z^s} + \chi_w^{(3)} \left[\frac{{\kappa_w}^2}{{\kappa_w}^2 + (\Delta k_z^w)^2} + \frac{i\Delta k_z^w \kappa_w}{{\kappa_w}^2 + (\Delta k_z^w)^2} \right] \right) \Phi_w(0) \qquad (15)$$

Here, the bulk silica $\chi^{(3)}$ contribution is expressed with $i\chi_s^{(3)} \frac{\kappa_w(\varepsilon_r^w / \varepsilon_r^s)}{\Delta k_z^s} \Phi_w(0)$. This is a pure imaginary term, and its amplitude is many times of that for the bulk water $\chi^{(3)}$ contribution. To see this, one can plug in the values of Debye screening length $1/\kappa_w$ (1nm for 0.1M NaCl), SHG coherent length in bulk silica ($1/\Delta k_z^s$ =20 nm), and in bulk water ($1/\Delta k_z^w$ =26.5 nm), ε_r^s (4), and ε_r^w (78.54) to eq 15, one has $i392.7\chi_s^{(3)}\Phi_w(0)$. Since bulk $\chi_s^{(3)}$ (=3.11 esu) and $\chi_w^{(3)}$ (=2.80 esu) values are close,[28] then $392.7\chi_s^{(3)} = 436.2\chi_w^{(3)}$. These values are listed in Table 1 and shown in Figure 2. Therefore, $i\chi_s^{(3)} \frac{\kappa_w(\varepsilon_r^w / \varepsilon_r^s)}{\Delta k_z^s} \Phi_w(0) = i436.2\chi_w^{(3)}\Phi_w(0)$. In comparison, the bulk water term in eq 13 gives $\frac{1}{1-i/26.5}\chi_w^{(3)}\Phi_w(0)$, and its amplitude is $0.999\chi_w^{(3)}\Phi_w(0)$. This indeed gives a more than 400 times larger $\chi^{(3)}$ contribution for the bulk silica over that of the bulk water phase, providing a qualitatively explanation of the EFISHG intensity data for the charged silica/water interface and the air/water interface.[1-3] However, a more than 400 time larger bulk silica $\chi^{(3)}$ contribution over that of the bulk water is probably a significant over-estimation of the bulk silica $\chi^{(3)}$ contribution. The cause of the over-estimation is most likely the overlook of the effects of the charge screening in the bulk water phase on the electric field in the bulk silica phase. Nevertheless, this scenario does show that the bulk silica $\chi^{(3)}$ contribution may dominate the EFISHG from the charged silica/water interface, a reasonable explanation for the EFISHG data discussed above.[1-3]

Table 1. Dielectric and nonlinear parameters for fused silica and water.

Material	ε_r	n_{bulk} (mol/cm^3)	γ^e (10^{-36} esu)	μ (D)	β (10^{-38} esu)	$\chi^{(3)}$ (10^{-14} esu)
Fused silica	~ 4	0.0367	4.02[28]	0.5[29]	—	3.11[28], 3.5[30-31]
Water	78.54[32]	0.0556	0.83[28] , 0.91[33]	2.95-2.98[34-35]	1.62[33]	2.80[28]

[30]Measured by THG at 1064 nm. [28, 31, 33] Measured by EFISHG at 1064 nm.

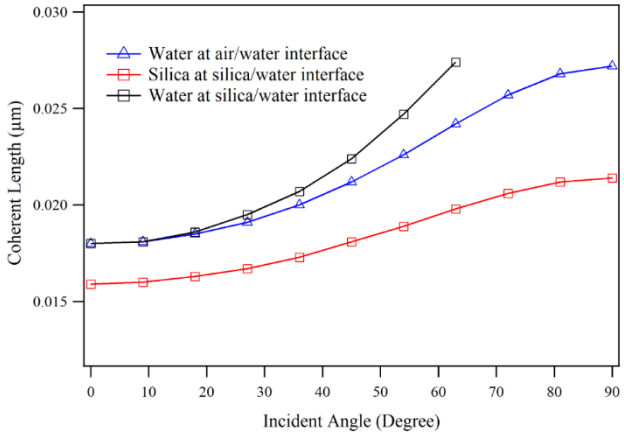

Figure 2. Incident angle dependent SHG coherent length ($1/\Delta k_z$) in water and silica with E_ω=600 nm. Blue and Black: for water of air/water and silica/water interfaces, respectively; Red: for silica of silica/water interfaces. For silica/water interface, 62.45° is the total internal reflection (TIR) angle.

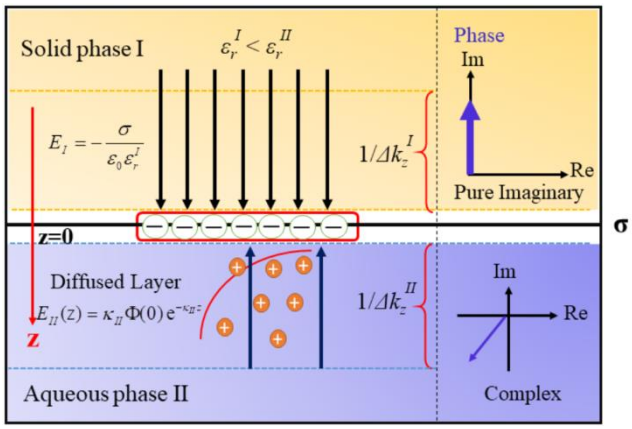

Figure 3. The electric fields on both sides of the interface for negative charged interface with interfacial charge density σ. In solids phase I, electric field is constant and inversely proportional to the dielectric constant ε_r^I; for aqueous phase II, electric field is $E_{II}(z) = -\kappa_{II}\Phi(0)e^{-\kappa_{II}z}$ as the result of charge screening (orange circle). $1/\Delta k_z^i$ is the coherent length.

The resulted bulk water phase contribution is a complex quantity.

In the second scenario, the effects of the charge screening in the water phase need to be included, and this is expected to reduce the value of the $\chi^{(3)}$ contributions from the bulk silica phase.

The effects of the charge screening in the water phase on the bulk silica $\chi^{(3)}$ contributions can be treated with the image charge distribution of the charge distribution in the bulk water phase. This shall make the electric field $E_s^0(z)$ in the bulk silica phase in eq 10 distance-dependent, i.e., z dependent. Therefore, with $\Phi_s(z) = \Phi_s(0)e^{-\kappa_s|z|}$, following the same calculation with the eq 13, eq 10 and eq 11 gives,

$$\begin{aligned}\chi_{s,eff}^{(3)} &= -\chi_s^{(3)} \frac{\kappa_s}{\kappa_s - i\Delta k_z^s} \Phi_s(0) \\ &= -\chi_s^{(3)} \left[\frac{\kappa_s^{\,2}}{\kappa_s^{\,2} + (\Delta k_z^s)^2} + \frac{i\Delta k_z^s \kappa_s}{\kappa_s^{\,2} + (\Delta k_z^s)^2} \right] \Phi_s(0)\end{aligned} \tag{16}$$

Now one needs to evaluate the κ_s, and the $\Phi_s(0)$ terms in this equation.

Following the Gauss Theorem, one has $\varepsilon_r^s E_0^s(0) = \varepsilon_r^w E_0^w(0)$, i.e., $\varepsilon_r^s \kappa_s \Phi_s(0) = \varepsilon_r^w \kappa_w \Phi_w(0)$. Then,

$$\chi_{eff}^{(2)} = \chi^{(2)} + \left(-\chi_s^{(3)} \frac{\kappa_s}{\kappa_s - i\Delta k_z^s} \frac{\varepsilon_r^w \kappa_w}{\varepsilon_r^s \kappa_s} + \chi_w^{(3)} \frac{\kappa_w}{\kappa_w - i\Delta k_z^w} \right) \Phi_w(0) \tag{17}$$

Here eq 17 gives the description of the $\chi^{(3)}$ contributions from both the bulk water and silica phases. It is important to note that according to eq 17, the bulk silica phase $\chi^{(3)}$ contribution term $-\chi_s^{(3)} \frac{\kappa_s}{\kappa_s - i\Delta k_z^s} \frac{\varepsilon_r^w \kappa_w}{\varepsilon_r^s \kappa_s}$ is no longer pure imaginary. It has become with the same form as that form the bulk water $\chi^{(3)}$ contributions, but much larger amplitude.

The expression for the Debye screening length $1/\kappa_w$ (in CGS unit) in water with electrolyte ion (with ion charge of $z_{i,w}$) and concentration of $\rho_{\infty i}$ is, [36]

$$\kappa_w = \left(\sum_i \rho_{\infty i}^w e^2 z_{i,w}^2 \Big/ \varepsilon_0 \varepsilon_r^w kT \right)^{1/2} \tag{18}$$

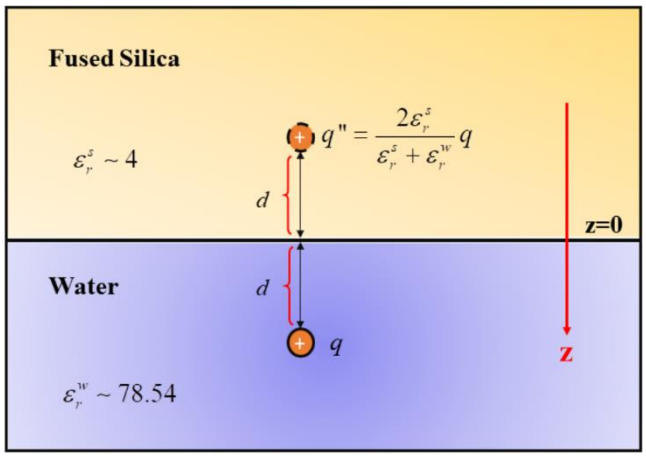

Figure 4. The image charge q'' in bulk silica phase resulted from the charge q in bulk water phase. d is the distance from the charge to interface (z=0). $q'' = 0.097q$.

The image charge distribution in the bulk silica phase determines the value of κ_s when the electrolyte ion distribution in water is known. As in Figure 4, considering a point charge q in water located at distance d apart from a plane separating the water and silica phases with,

$$\varepsilon(z) = \begin{cases} \varepsilon_r^s \sim 4 & for \quad z \in (-\infty, 0^-) \\ \varepsilon_r^w \sim 78.54 & for \quad z \in (0^+, +\infty) \end{cases} \tag{19}$$

Then, the image charge method gives the electric potentials inside the water and silica bulk phases generated by this point charge q, respectively as below,[37]

$$\Phi_w(z) = \frac{1}{4\pi\varepsilon_r^w} \left(\frac{q}{\sqrt{(z-d)^2}} + \frac{q'}{\sqrt{(z+d)^2}} \right) \quad z > 0 \tag{20}$$

$$\Phi_s(z) = \frac{1}{4\pi\varepsilon_r^s} \frac{q''}{\sqrt{(z-d)^2}} \quad z < 0 \tag{21}$$

with $q' = -q\frac{\varepsilon_r^s - \varepsilon_r^w}{\varepsilon_r^s + \varepsilon_r^w}$, $q'' = q\frac{2\varepsilon_r^s}{\varepsilon_r^w + \varepsilon_r^s}$. Here the q'' is the effective charge inside the silica phase at the same distance from the interface. With the known silica and water static dielectric values, one has $q'' = 0.097q$. Therefore, the Debye screening length $1/\kappa_s$ (in CGS unit) in silica can be calculated

using eq 18 with the same charge distribution as in the bulk water phase with the equivalent point charge of q'' with the electrolyte ion (with ion charge number of $z_{i,w}$) and concentration of $\rho_{\infty i}$, i.e.,

$$\kappa_s = \left(\sum_i \rho_{\infty i}^w q''^2 z_{i,w}^2 / \varepsilon_0 \varepsilon_r^s kT \right)^{1/2} \tag{22}$$

Therefore, from eqs 21 and 22, one has $\frac{\kappa_s}{\kappa_w} = \left(\frac{q''^2 \varepsilon_r^w}{e^2 \varepsilon_r^s} \right)^{1/2}$, i.e., $\kappa_s = 0.430 \kappa_w$. This suggests that the charge screening effects in the bulk silica phase is at the same order of that in the bulk phase, even though the image charge is only about 10% of the charge of the ions in the water phase. To be exact, they screening lengths are different by a factor of 1/0.430=2.33. Now, the Gauss boundary condition $\varepsilon_r^s \kappa_s \Phi_s(0) = \varepsilon_r^w \kappa_w \Phi_w(0)$ suggests that $\Phi_s(0) = \frac{\varepsilon_r^w \kappa_w}{\varepsilon_r^s \kappa_s} \Phi_w(0) = \frac{78.54}{4 \times 0.430} \Phi_w(0) = 45.7 \Phi_w(0)$, i.e., the surface potential on the silica side is 45.7 times of that for the water side. With these relationships, eq 17 becomes,

$$\chi_{eff}^{(2)} = \chi^{(2)} + \left(-50.7 \frac{\kappa_w}{\kappa_w - i2.33\Delta k_z^s} + \frac{\kappa_w}{\kappa_w - i\Delta k_z^w} \right) \chi_w^{(3)} \Phi_w(0) \tag{23}$$

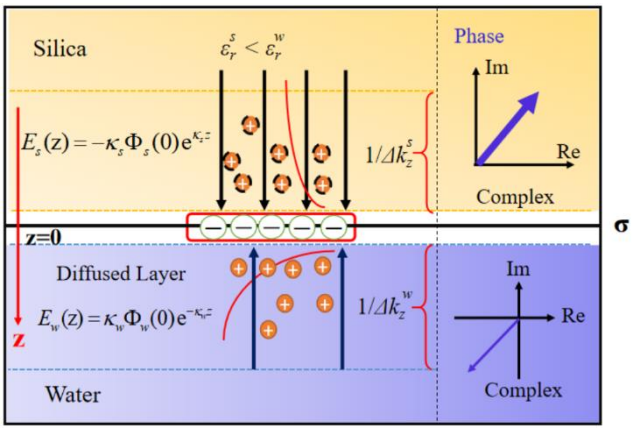

Figure 5. The electric fields on both sides of the interface for negative charged interface with interfacial charge density σ. The field in bulk silica is $E_s = -\kappa_s \Phi_s(0) e^{-\kappa_s z}$ when the image charge screening is considered (dashed orange circle); The field in the water phase is $E_w = \kappa_w \Phi_w(0) e^{-\kappa_w z}$ with charge screening (orange circle). $1/\Delta k_z^i$ is the coherent length. The

resulted bulk contributions are both complex quantities.

Plug in the values of Debye screening length $1/\kappa_w$ (1nm for 0.1M NaCl), SHG coherent length in bulk silica ($1/\Delta k_z^s$ =20 nm), and in bulk water ($1/\Delta k_z^w$ =26.5 nm), ε_r^s (4), ε_r^w (78.54), $\chi_s^{(3)}$ (=3.11 esu) and $\chi_w^{(3)}$ (=2.80 esu) values to eq 23, one has.

$$\begin{aligned}&\left(-50.7\frac{\kappa_w}{\kappa_w - i2.33\Delta k_z^s}+\frac{\kappa_w}{\kappa_w - i\Delta k_z^w}\right)\chi_w^{(3)}\Phi_w(0)\\&=\left(-50.7\times\frac{1}{1-i/8.6}+\frac{1}{1-i/26.5}\right)\chi_w^{(3)}\Phi_w(0)\end{aligned} \tag{23}$$

Therefore, the ratio of the amplitudes from bulk silica and bulk water contributions are 50.4:1. From eq 23, one can also see that when Δk_z^s *and* $\Delta k_z^w \gg \kappa_w$, both the bulk silica and water $\chi^{(3)}$ contributions are to be pure imaginary, then their amplitude ratio is going to be 21.8:1. This indicates that the overall amplitude of the bulk silica contribution is about 50 to 20 times of that from the bulk water contribution, with both terms to be complex, and close to real when the charge screening is strong, and close to pure imaginary when the charge screening is negligible. Such amplitude difference of about 50 to 20 times difference between the bulk silica and water $\chi^{(3)}$ contributions is much smaller than the over 400 times difference as predicted from eq 15, which did not consider the charge screening effects of the image charge in the bulk silica phase. Therefore, eq 17 is more quantitatively consistent with the EFISHG data from the silica/water interface as discussed above.[1-3]

Here, the bulk silica contribution term in eq 17 is completely different from those in eqs 8 and 15. In eqs 8 and 15, the bulk $\chi^{(3)}$ contributions from the bulk silica are completely imaginary; while in eq 17, this contribution is not only complex, but also can be almost real when the charge screening is significant. Also, since $\kappa_s = 0.430\kappa_w$, which means that the Debye screening length in bulk silica is always 2.33 times of that for the bulk water phase, the imaginary component of the bulk silica term is always bigger than that of the bulk water term.

According to eqs 17 and 23, the bulk silica $\chi^{(3)}$ contributions is complex and cannot be treated as purely imaginary in most cases. An attempt of doing so to account for the phase-resolved EFISHG measurements quantitatively did not work out,[15] leaving the origin of the new imaginary term as an open question. To compare eq 17 with eq 3, where a new pure imaginary term is proposed for description of the EFISHG of the silica/water interface, the two equations cannot be consistent with each other. Even though eq 15 does give the pure imaginary term from the bulk silica contribution, the treatment does not include the charge screening effects and the predicted amplitude of the bulk silica contribution is unreasonably high. Therefore, one would conclude that more detailed comparison between the eq 17 and the phase resolved EFISHG experimental data on the charged silica/water interface is expected in the future studies.

4. CONCLUSIONS

In this report, the $\chi^{(3)}$ contributions from the bulk silica phase to the EFISHG of the silica/water interface is added into the existing treatment that only included the bulk water phase $\chi^{(3)}$ contributions. The significantly different EFISHG signal intensity for the charged silica/water interface and air/water interface can be successfully interpreted using the proposed treatment.

Three models are considered from the simplest to more realistic. Namely, a) to treat both bulk phase as lossless dielectric bulk phase without considering charge screening effects induced by the interface charge; b) to treat the bulk silica phase as lossless dielectric bulk phase without considering charge screening, while treat the bulk water phase as electrolyte solution with charge screening effects; and c) to treat both the bulk silica and water phases with charge screening effects.

In all three cases, the electric field discontinuity across the interface dictated by the Gauss

Theorem of electromagnetics is responsible for the dominant contribution to the EFISHG signal from the bulk silica phase $\chi^{(3)}$ contributions over that from the bulk water phase, a result of the significantly different dielectric constants of the two bulk phases. However, only by including the image charge screening of the charge distribution in the water phase to the electric field inside the bulk silica phase can successfully provide a quantitatively reasonable interpretation for the different EFISHG signal for the charged silica/water and air/water interfaces. One possible way to test the effectiveness of the treatment, particularly the image charge screening effects on the electric fields inside the bulk silica phase, is to mix in water with water soluble solvents to tune the dielectric constant of the electrolyte solution phase, then to see how this would affect the phase resolved EFISHG response. The fact that the EFISHG of the silica/water interface is dominated by the bulk silica $\chi^{(3)}$ contributions, which are complete absent in the EFISFG-VS of the silica/water interface make it easy to understand why the EFISHG and EFISFG-VS data are not always consistent with each other as Hore, and Gibbs *et al.* pointed out fairly recently.[4]

According to these treatments discussed in this report, the electric field discontinuity across the interface at high interfacial charge density can create a huge potential difference across the interface. The fully charged silica/water interface at high pH can have $\Phi_w(0) \sim 140mV$,[1-2] then $\Phi_s(0) = 45.7\Phi_w(0) \sim 6400mV$. If the thickness of the silica/water interface is 1nm, this corresponds to a field across the interface as high as 6.3×10^9 V/m. To sustain such a high electric field across the interface, the structure of molecules at the interface would be significantly affected. How the structures at the interface would be different from neutral to highly charged condition need to be studied. So far, the interface is only treated as a sheet of charge with a density of σ in our model. More realistic model needs to consider the structural changes of the interface itself. The thickness of

the interface might be increased under high charge density. Such information is certainly important for designing electrode materials. Nevertheless, the EFISHG properly studied may help reveal these differences.

The models treated in this report do confirm the ability to use EFISHG to determine interfacial potentials of a giving interface. No matter the EFISHG signal dominated by the $\chi^{(3)}$ contributions from bulk silica or bulk water phases, they do follow similar forms and they are both proportional to the amplitude of the interfacial potential $\Phi_w(0)$, with different $\chi^{(3)}$ values. This is also why it worked well in making measurement of the interfacial potential and the pKa of the acid-base equilibrium at the air/water interfaces.[1-3]

The models and concepts discussed in this report may also be used to treat other type of charged interfaces. The dielectric properties of the bulk phases, the charge distribution and screening effects can be measured with EFISHG from those interfaces, and different models to describe each contribution to the SHG susceptibility can be tested.

5. AUTHOR INFORMATION

Corresponding Author: *(H.-F.W.) E-mail: wanghongfei@westlake.edu.cn.

ORCID: Hong-Fei Wang: 0000-0001-8238-1641

Hui Wang: 0000-0003-1039-7833

Xiao-Hua Hu: 0000-0002-4839-5000

Notes:

The authors declare no competing financial interest.

6. ACKNOWLEDGEMENTS

We had insightful discussions with Franz Geiger on phase resolved EFISHG experimental results. H.F.W. thanks Congjun Wu for consultation on one physical detail. H.F.W. also thanks the support of National Natural Science Foundation of China (No.21727802).

REFERENCES

1. Ong, S.; Zhao, X.; Eisenthal, K. B., Polarization of Water Molecules at a Charged Interface: Second Harmonic Studies of the Silica/Water Interface. *Chem. Phys. Lett.* **1992**, *191*, 327-335.
2. Zhao, X.; Ong, S.; Eisenthal, K. B., Polarization of Water Molecules at a Charged Interface. Second Harmonic Studies of Charged Monolayers at the Air/Water Interface. *Chem. Phys. Lett.* **1993**, *202*, 513-520.
3. Zhao, X.; Ong, S.; Wang, H.; Eisenthal, K. B., New Method for Determination of Surface pKa Using Second Harmonic Generation. *Chem. Phys. Lett.* **1993**, *214*, 203-207.
4. Rehl, B.; Rashwan, M.; DeWalt-Kerian, E. L.; Jarisz, T. A.; Darlington, A. M.; Hore, D. K.; Gibbs, J. M., New Insights into X(3) Measurements: Comparing Nonresonant Second Harmonic Generation and Resonant Sum Frequency Generation at the Silica/Aqueous Electrolyte Interface. *J. Phys. Chem. C* **2019**, *123*, 10991-11000.
5. Wen, Y. C.; Zha, S.; Liu, X.; Yang, S.; Guo, P.; Shi, G.; Fang, H.; Shen, Y. R.; Tian, C., Unveiling Microscopic Structures of Charged Water Interfaces by Surface-Specific Vibrational Spectroscopy. *Phys Rev Lett* **2016**, *116*, 016101.
6. Gonella, G.; Lutgebaucks, C.; de Beer, A. G. F.; Roke, S., Second Harmonic and Sum-Frequency Generation from Aqueous Interfaces Is Modulated by Interference. *J. Phys. Chem. C* **2016**, *120*, 9165-9173.
7. Ohno, P. E.; Saslow, S. A.; Wang, H.-f.; Geiger, F. M.; Eisenthal, K. B., Phase-Referenced Nonlinear Spectroscopy of the α-Quartz/Water Interface. *Nat. Commun* **2016**, *7*, 13587.
8. Wang, H. F., Sum Frequency Generation Vibrational Spectroscopy (SFG-VS) for Complex Molecular Surfaces and Interfaces: Spectral Lineshape Measurement and Analysis Plus Some Controversial Issues. *Prog. Surf. Sci* **2016**, *91*, 155-182.
9. Ohno, P. E.; Wang, H.-f.; Geiger, F. M., Second-Order Spectral Lineshapes from Charged Interfaces. *Nat. Commun* **2017**, *8,*1032.
10. Ohno, P. E.; Wang, H.-f.; Paesani, F.; Skinner, J. L.; Geiger, F. M., Second-Order Vibrational Lineshapes from the Air/Water Interface. *J. Phys. Chem. A* **2018**, *122*, 4457-4464.
11. Reddy, S. K.; Thiraux, R.; Rudd, B. A. W.; Lin, L.; Adel, T.; Joutsuka, T.; Geiger, F. M.; Allen, H. C.; Morita, A.; Paesani, F., Bulk Contributions Modulate the Sum-Frequency Generation Spectra of Water on Model Sea-Spray Aerosols. *Chem* **2018**, *4*, 1629-1644.
12. Ohno, P. E.; Chang, H.; Spencer, A. P.; Liu, Y.; Boamah, M. D.; Wang, H.-f.; Geiger, F. M., Beyond the Gouy-Chapman Model with Heterodyne-Detected Second Harmonic Generation. *J. Phys. Chem. Lett* **2019**, *10*, 2328-2334.
13. Ma, E.; Kim, J.; Chang, H.; Ohno, P. E.; Jodts, R. J.; Miller, T. F., III; Geiger, F. M., Stern and Diffuse Layer Interactions During Ionic Strength Cycling. *J. Phys. Chem. C* **2021**, *125*, 18002-18014.
14. Rehl, B.; Gibbs, J. M., Role of Ions on the Surface-Bound Water Structure at the Silica/Water Interface: Identifying the Spectral Signature of Stability. *J. Phys. Chem. Lett* **2021**, *12*, 2854-2864.
15. Ma, E.; Ohno, P. E.; Kim, J.; Liu, Y.; Lozier, E. H.; Miller, T. F., III; Wang, H.-F.; Geiger, F. M., A New Imaginary Term in the Second-Order Nonlinear Susceptibility from Charged Interfaces. *J. Phys. Chem. Lett* **2021**, *12*, 5649-5659.
16. Geiger, F. M., Second Harmonic Generation, Sum Frequency Generation, and χ((3)): Dissecting Environmental Interfaces with a Nonlinear Optical Swiss Army Knife. *Annu. Rev. Phys. Chem*, **2009**, *60*, 61-83.
17. Byrnes, S. J.; Geissler, P. L.; Shen, Y. R., Ambiguities in Surface Nonlinear Spectroscopy Calculations. *Chem. Phys. Lett.* **2011**, *516*, 115-124.
18. Konek, C. T.; Musorrafiti, M. J.; Al-Abadleh, H. A.; Bertin, P. A.; Nguyen, S. T.; Geiger, F. M., Interfacial Acidities, Charge Densities, Potentials, and Energies of Carboxylic Acid-Functionalized Silica/Water Interfaces Determined by Second Harmonic Generation. *J. Am. Chem. Soc.* **2004**, *126*, 11754-11755.
19. Hayes, P. L.; Chen, E. H.; Achtyl, J. L.; Geiger, F. M., An Optical Voltmeter for Studying Cetyltrimethylammonium Interacting with Fused Silica/Aqueous Interfaces at High Ionic Strength. *J. Phys. Chem. A* **2009**, *113*, 4269-80.

20. Darlington, A. M.; Gibbs-Davis, J. M., Bimodal or Trimodal? The Influence of Starting pH on Site Identity and Distribution at the Low Salt Aqueous/Silica Interface. *J. Phys. Chem. C* **2015**, *119*, 16560-16567.

21. Myalitsin, A.; Urashirna, S. H.; Nihonyanagi, S.; Yamaguchi, S.; Tahara, T., Water Structure at the Buried Silica/Aqueous Interface Studied by Heterodyne-Detected Vibrational Sum-Frequency Generation. *J. Phys. Chem. C* **2016**, *120*, 9357-9363.

22. Azam, M. S.; Cai, C.; Gibbs, J. M.; Tyrode, E.; Hore, D. K., Silica Surface Charge Enhancement at Elevated Temperatures Revealed by Interfacial Water Signals. *J. Am. Chem. Soc.* **2020**, *142*, 669-673.

23. Rashwan, M.; Rehl, B.; Sthoer, A.; Darlington, A. M.; Azam, M. S.; Zeng, H.; Liu, Q.; Tyrode, E.; Gibbs, J. M., Structure of the Silica/Divalent Electrolyte Interface: Molecular Insight into Charge Inversion with Increasing pH. *J. Phys. Chem. C* **2020**, *124*, 26973-26981.

24. Jena, K. C.; Hore, D. K., Variation of Ionic Strength Reveals the Interfacial Water Structure at a Charged Mineral Surface. *J. Phys. Chem. C* **2009**, *113*, 15364-15372.

25. Jena, K. C.; Covert, P. A.; Hore, D. K., The Effect of Salt on the Water Structure at a Charged Solid Surface: Differentiating Second- and Third-Order Nonlinear Contributions. *J. Phys. Chem. Lett* **2011**, *2*, 1056-1061.

26. Darlington, A. M.; Jarisz, T. A.; DeWalt-Kerian, E. L.; Roy, S.; Kim, S.; Azam, M. S.; Hore, D. K.; Gibbs, J. M., Separating the Ph-Dependent Behavior of Water in the Stern and Diffuse Layers with Varying Salt Concentration. *J. Phys. Chem. C* **2017**, *121*, 20229-20241.

27. Hore, D. K.; Tyrode, E. C., Probing Charged Aqueous Interfaces near Critical Angles: Effect of Varying Coherence Length. *J. Phys. Chem. C* **2019**.

28. Kajzar, F.; Messier, J., Third-Harmonic Generation in Liquids. *Phys. Rev. A. Gen. Phys* **1985**, *32*, 2352-2363.

29. Golding, B.; Schickfus, M. V.; Hunklinger, S.; Dransfeld, K., Intrinsic Electric-Dipole Moment of Tunneling Systems in Silica Glasses. *Phys. Rev. Lett* **1979**, *43*, 1817-1821.

30. Kajzar, F., Electric Field Induced Second Harmonic Generation. *Proc. of SPIE* **1997**, *480*, 10291P.

31. Nasu, H.; Matsuoka, J.; Kamiya, K., Second- and Third-Order Optical Non-Linearity of Homogeneous Glasses. *J. Non-Cryst. Solids* **1994**, *178*, 23-30.

32. Sylvester-Hvid, K. O.; Mikkelsen, K. V.; Norman, P.; Jonsson, D.; Ågren, H., Sign Change of Hyperpolarizabilities of Solvated Water, Revised: Effects of Equilibrium and Nonequilibrium Solvation. *J. Phys. Chem. A* **2004**, *108*, 8961-8965.

33. Kaatz, P.; Donley, E. A.; Shelton, D. P., A Comparison of Molecular Hyperpolarizabilities from Gas and Liquid Phase Measurements. *J.Chem. Phys.* **1998**, *108*, 849-856.

34. Silvestrelli, P. L.; Parrinello, M., Water Molecule Dipole in the Gas and in the Liquid Phase. *Phys. Rev. Lett* **1999**, *82*, 3308-3311.

35. Gubskaya, A. V.; Kusalik, P. G., The Total Molecular Dipole Moment for Liquid Water. *J. Chem. Phys* **2002**, *117*, 5290-5302.

36. N.Israelachvili, J., *Intermolecular and Surface Forces, Elsevier (third edition)*, p293.

37. Lacava, F., *Classical Electrodynamics, Springer(first edition)*, p55.